PCCP

COMMUNICATION

View Article Online
View Journal | View Issue

Cite this: *Phys. Chem. Chem. Phys.*, 2015, **17**, 8633

Received 28th January 2015,
Accepted 3rd March 2015

DOI: 10.1039/c5cp00536a

www.rsc.org/pccp

Solvent-dependent structure of molecular iodine probed by picosecond X-ray solution scattering†

Kyung Hwan Kim,[ab] Hosung Ki,[ab] Jae Hyuk Lee,‡[b] Sungjun Park,[ab] Qingyu Kong,§[c] Jeongho Kim,[d] Joonghan Kim,*[e] Michael Wulff[c] and Hyotcherl Ihee*[ab]

The effect of solute–solvent interaction on molecular structure and reaction dynamics has been a target of intense studies in solution-phase chemistry, but it is often challenging to characterize the subtle effect of solute–solvent interaction even for the simplest diatomic molecules. Since the I_2 molecule has only one structural parameter and exhibits solvatochromism, it is a good model system for investigating the solvent dependence of the solute structure. By using X-rays as a probe, time-resolved X-ray liquidography (TRXL) can directly elucidate the structures of reacting molecules in solution and can thus determine the solvent-dependent structural change with atomic resolution. Here, by applying TRXL, we characterized the molecular structure of I_2 in methanol and cyclohexane with sub-angstrom accuracy. Specifically, we found that the I–I bond length of I_2 is longer in the polar solvent (methanol) by ~0.2 Å than in nonpolar solvents (cyclohexane and CCl_4). Density functional theory (DFT) using 22 explicit methanol molecules well reproduces the longer I–I bond of molecular iodine in methanol and reveals that the larger bond length originates from partial negative charge filled in an antibonding σ* orbital through solvent-to-solute charge transfer.

For chemical reactions in solution, the solvent serves as an energy source for activating a chemical reaction and a heat bath to stabilize the reaction products. In particular, solute molecules interact with surrounding solvent molecules constantly and the chemical properties of the solvent often alter the molecular structure and dynamics by changing the landscape of the potential energy surface. Although the effect of solute–solvent interaction on molecular structure and chemical reactions has been a target of intense studies,[1–6] it is challenging to characterize the subtle effects of solute–solvent interaction, even for the simplest diatomic molecules.

Molecular iodine (I_2) has a simple structure with only one variable, the I–I bond length, and can serve as a good model system for investigating the effect of solute–solvent interaction. In particular, I_2 in solution exhibits solvatochromism,[7–9] which means that the absorption spectrum is spectrally shifted due to a change in solvent polarity. For example, Fig. S1 in the ESI† shows that the absorption spectrum of I_2 in methanol is distinctly different from the ones in nonpolar solvents (cyclohexane and CCl_4), demonstrating the strong influence of the solute–solvent interaction on the electronic properties of the solute molecules. Previously, the solvatochromism of I_2 was explained by the formation of a charge transfer complex induced by solvent-to-solute electron transfer.[10] Despite many experimental and theoretical studies,[11–16] the validity of that model as well as the molecular origin of the solvatochromism is still an open question. Considering the simple structure of I_2, electronic properties such as the absorption spectrum must be strongly correlated with its single structural parameter, the I–I bond length. Thus, in order to have a molecular-level understanding of the solvatochromism of I_2 in solution, it would be essential to characterize the variation of the I–I bond length in various solvents exhibiting solvatochromism. However, it is difficult to extract the exact length of the I–I bond from the absorption spectrum because the absorption spectrum is affected by a complex interplay of electronic correlations and spin–orbit coupling. In effect, the change in molecular structure might often be small even for large changes in the absorption spectrum.

In contrast, structural probes based on X-rays or electrons, for example X-ray absorption[17–19] and X-ray or electron diffraction (scattering),[20,21] can provide direct information on the global molecular structure. In fact, static X-ray scattering was used to characterize the molecular structure of I_2 in gas and solid

[a] *Center for Nanomaterials and Chemical Reactions, Institute for Basic Science (IBS), Daejeon 305-701, Republic of Korea. E-mail: hyotcherl.ihee@kaist.ac.kr; Fax: +82-42-350-2810; Tel: +82-42-350-2884*
[b] *Department of Chemistry, KAIST, Daejeon 305-701, Republic of Korea*
[c] *European Synchrotron Radiation Facility, BP 220, 38043 Grenoble Cedex, France*
[d] *Department of Chemistry, Inha University, Incheon 402-751, Republic of Korea*
[e] *Department of Chemistry, The Catholic University of Korea, Bucheon 420-743, Republic of Korea. E-mail: joonghankim@catholic.ac.kr*

† Electronic supplementary information (ESI) available. See DOI: 10.1039/c5cp00536a

‡ Present address: Ultrafast X-ray Science Laboratory, Lawrence Berkeley National Laboratory, Berkeley, CA 94720, USA.
§ Present address: X-ray Science Division, Argonne National Laboratory, 9700 S. Cass Avenue, Argonne, IL 60439, USA.

phase accurately,[22] but it could not be applied to dilute solutions because of the large background signal from the dominating contributions of solvent molecules. Also, X-ray absorption spectroscopy in the EXAFS region was applied to I_2 in solution,[15] but it failed to resolve any significant solvent-dependent change in the molecular structure of I_2, probably due to incorrect solvent corrections in the model used to fit the data.

In this work, we apply time-resolved X-ray liquidography (TRXL) to the photodissociation of I_2 in two different solvents (methanol and cyclohexane) to investigate the effect of solute–solvent interaction on the molecular structure of I_2 in the ground state. TRXL makes use of a pump–probe scheme with a visible-light pump and an X-ray scattering probe which can effectively determine the molecular structures in the solution phase. With the sub-Å spatial resolution and 100 picosecond temporal resolution from 3rd-generation synchrotrons, TRXL has been used for revealing structural dynamics and mechanism of various molecular reaction systems ranging from small molecules[23–28] to biological macromolecules.[29–32] By comparing the ground-state structures of I_2 (the reactant in the photodissociation) in methanol and cyclohexane, determined from TRXL, we elucidate the effect of solute–solvent interaction on the molecular structure.

The principle of the TRXL experiment is shown schematically in Fig. 1 with the details described in the ESI.† Briefly, a ~2 ps laser pulse initiates the photodissociation of I_2 molecules in methanol and cyclohexane with the center wavelength of 400 nm and 520 nm, respectively, and a time-delayed X-ray pulse of ~100 ps duration monitors the progress of the reaction. To explore the solvent dependence of the molecular structure of I_2, we used samples of I_2 in two different solvents (methanol and cyclohexane) at 10 mM concentration. Scattering patterns from I_2 solutions were measured before (at −5 ns time delay) and after laser excitation, and the patterns were subtracted from each other to remove the background from non-reacting molecules. The resultant difference scattering patterns contain the information only on the molecular structural changes induced by the photoinduced reaction.

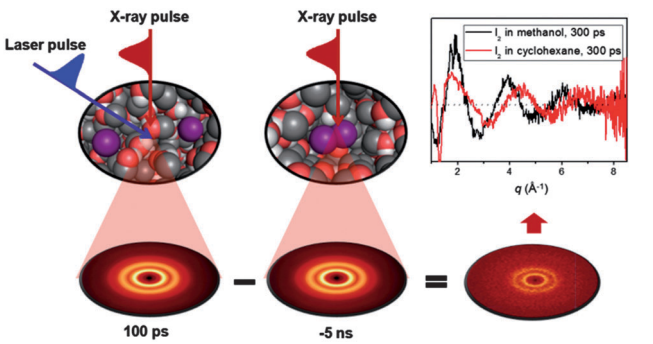

Fig. 1 Schematic of the TRXL experiment. Scattering patterns from I_2 solution are measured before and after laser excitation and the patterns are subtracted from each other to obtain the difference scattering patterns, which contain only information on the activated molecules in the reaction. To explore the solvent dependence of the molecular structure of I_2, we used solution samples in two different solvents (methanol and cyclohexane).

TRXL has been mainly used for investigating the structural dynamics of reaction intermediates and products, but it can also probe the structures of the reactants[33] since the scattering pattern from the negative time delay probes the reactants (or initial states). For the structural analysis, the difference scattering curves were fitted by theoretical curves using maximum likelihood estimation (MLE) with a chi-square estimator.[34] The theoretical difference curves of the solution sample have three components: (i) the solute-only term, (ii) the solute–solvent cross term, and (iii) the solvent-only term. The solute-only term is calculated by the Debye equation,

$$S(q) = F_I^2(q)\frac{\sin qR_{I-I}}{qR_{I-I}}$$

where F_I is the atomic form factor of an iodine atom and R_{I-I} is the I–I distance. In the fitting analysis, R_{I-I} was used as a free parameter to determine the molecular structure of I_2 accurately. More details on the analysis method are given in the ESI† and in our previous publications.[24,26,33,34]

According to previous studies of the photodissociation of I_2 in solution using time-resolved spectroscopy[35,36] and TRXL,[37,38] the photodissociated iodine atoms recombine either geminately (by relaxation through the A/A′ state or *via* vibrational cooling in the X state) or nongeminately (by slow diffusion). Since we aim to probe the molecular structure of I_2 in the ground state in this work, it is desirable to eliminate the contributions of geminate recombination to the TRXL signal. We therefore analyzed the TRXL data on the time scales covering both geminate and nongeminate recombination and found that the lifetimes of A/A′ state and vibrationally hot X state are much shorter than 100 ps in both methanol (see the ESI†) and cyclohexane.[37] Therefore, to determine the exact ground-state structure of I_2 in methanol and cyclohexane, we used the difference scattering curves at 300 ps time delay that do not have any contribution from the A/A′ state or from the vibrationally hot X state.

As shown in Fig. 1 (upper right panel), the difference scattering from the methanol and the cyclohexane solutions at 300 ps time delay exhibit oscillation periods that are different from each other, implying that the molecular structure of I_2 varies depending on the solvent. In order to extract the exact molecular structure of I_2 in the ground state, we performed the structural analysis of the experimental scattering curves at 300 ps as described in the ESI.† The results for I_2 in methanol are shown in Fig. 2. To emphasize only the contribution from the I–I pair in I_2, we extracted the solute-only term from the difference scattering curve of the solution sample (see the ESI† for details). For I_2 in methanol, the best fit of the scattering curve was obtained with the I–I bond length of 2.85 (±0.04) Å (χ^2 = 1.42) as can be seen in Fig. 2a. Alternatively, we tried to build the theoretical difference scattering curve using the I–I bond length of I_2 in CCl_4 (2.67 Å), determined in our previous TRXL study,[37] and compared it with the experimental difference scattering curve. As shown in Fig. 2a, the fitting quality deteriorates significantly (χ^2 = 3.29) with the I–I bond length of 2.67 Å.

To obtain a more intuitive picture of the molecular structure, we converted the difference scattering curves in q-space into

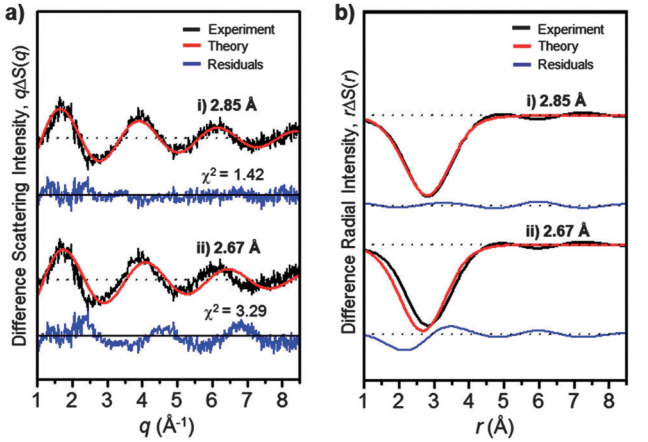

Fig. 2 Determination of the ground-state structure of I_2 in methanol in (a) q-space and (b) r-space. (a) Solute-only term of the experimental difference scattering curve at 300 ps (black) and theoretical difference scattering curve (red) built with I–I bond lengths of (i) 2.85 Å and (ii) 2.67 Å. (b) Radial distribution function, $r\Delta S(r,t)$, of the solute-only term built with I–I bond lengths of (i) 2.85 Å and (ii) 2.67 Å. The experimental difference scattering curve of I_2 in methanol is best fit by the theoretical scattering curve built with an I–I bond length of 2.85 Å.

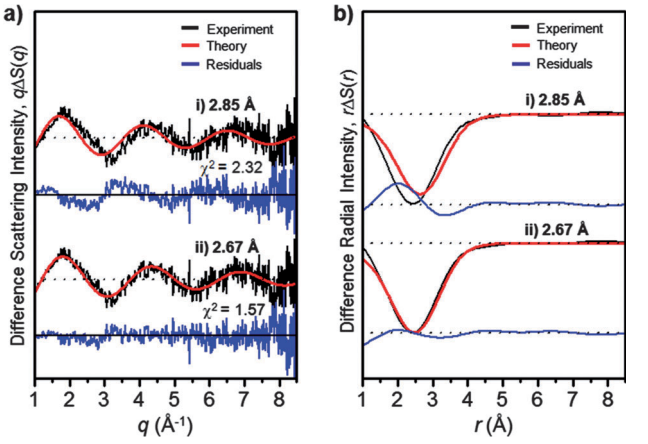

Fig. 3 Determination of the ground-state structure of I_2 in cyclohexane in (a) q-space and (b) r-space. (a) Solute-only term of the experimental difference scattering curve at 300 ps (black) and theoretical difference scattering curve (red) built with I–I bond lengths of (i) 2.85 Å and (ii) 2.67 Å. (b) Radial distribution function, $r\Delta S(r,t)$, of the solute-only term built with I–I bond lengths of (i) 2.85 Å and (ii) 2.67 Å. The experimental difference scattering curve of I_2 in cyclohexane is best fit by the theoretical scattering curve built with an I–I bond length of 2.67 Å.

difference radial distribution functions (RDFs), $r\Delta S(r,t)$, as shown in Fig. 2b. In principle, the solute-only term at 300 ps is supposed to contain only the contribution from the depletion of the reactant (I_2 in the ground state) because geminate recombination or photodissociation of I_2 into free iodine atoms is completed during that time delay. Therefore, there is only a single negative feature in the difference RDF, and the peak position of the negative feature directly represents the I–I bond length of I_2 in the ground state. In agreement with the fitting result in q-space, the experimental RDF has a negative feature peaked at r = 2.85 Å, which corresponds to the I–I bond length of I_2 in methanol.

The results of the structural fitting analysis for I_2 in cyclohexane are shown in Fig. 3. As can be seen in Fig. 3a, the best fit for I_2 in cyclohexane is obtained with the I–I bond length of 2.67 (±0.06) Å (χ^2 = 1.57), which is identical to that in another nonpolar solvent, CCl_4.[37] In contrast, the fitting quality becomes much worse (χ^2 = 2.32) when we use the I–I bond length of 2.85 Å, the bond length of I_2 in methanol.

On the basis of the structural fitting of the TRXL data presented above, we characterized the structure of the ground-state I_2 in two solvents with different polarities (methanol and cyclohexane) and elucidated the subtle structural variation of I_2 resulting from the change in the solute–solvent interaction. Specifically, we found that the I–I bond of I_2 is longer in a polar solvent (methanol) by ~0.2 Å than in nonpolar solvents (cyclohexane and CCl_4). To understand the molecular-level origin of the increased I–I bond length in methanol observed in the TRXL experiment, we performed a quantum chemical calculation using the density functional theory (DFT). Computational details of the calculation are described in the ESI.† In the quantum chemical calculations, the solvent environment is generally considered implicitly *via* the polarizable continuum model (PCM). Although the PCM reduces the computational costs and has been successfully applied to many molecular systems for decades, it may not be appropriate for describing the subtle effect of the solute–solvent interaction on the solute structure.[33] In fact, we obtained the optimized structure of I_2 with an I–I bond length of 2.67 Å in methanol when we considered the solvent environment implicitly by using the integral-equation-formalism polarizable continuum model (IEFPCM). This value is identical to the I–I bond length of I_2 in nonpolar solvents and disagrees with our TRXL measurement (2.85 Å), suggesting that the implicit treatment of the solvent environment does not properly describe the subtle change in the structure of I_2 arising from the change in solute–solvent interaction.

To better describe the solute–solvent interaction, we optimized the molecular structure of I_2 by treating the solvent molecules explicitly. Specifically, a total of 22 methanol molecules were used to form the first solvation shell around an I_2 molecule. As shown in Fig. 4, in the explicit solvent environment, we obtained the optimized structure of I_2 with a bond length of 2.73 Å, which is larger than the value for I_2 in nonpolar solvents (2.67 Å) or the one obtained with the implicit solvent model. The longer I–I bond in methanol is in agreement with the result of our TRXL measurement. To further validate this result, we calculated the potential energy curve of I_2 in methanol while varying the I–I bond length. As shown in Fig. 4, we confirmed that the optimized structure is located at the global minimum of the potential energy curve of I_2 in methanol. Also, the potential energy curve of I_2 in methanol has a larger width than the one calculated for an isolated I_2 molecule, which has a minimum at 2.67 Å, as shown in Fig. S5 in the ESI.† As a result, I_2 in methanol can vibrate with larger amplitude than the isolated molecule, confirming the presence of a weaker and hence a longer I–I bond in methanol than in nonpolar solvents.

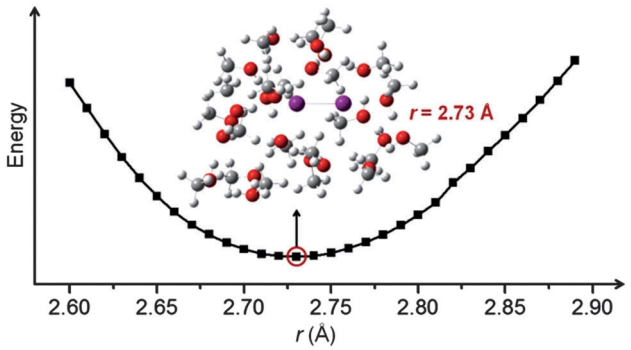

Fig. 4 Optimized structure of I_2 and its relative energy calculated by the DFT method. A total of 22 methanol molecules were used to form the first solvation shell around an I_2 molecule. The optimized structure of I_2 in methanol has an I–I bond of length 2.73 Å and is located at the global minimum of the potential energy curve. The iodine atoms in the optimized structure have partial charges of −0.19 and +0.12.

From the quantum chemical calculations we can infer the molecular origin of the larger bond length in methanol as arising from charge transfer from solvent molecules to I_2. Notably, the natural population analysis shows that I_2 in the solvation configuration shown in Fig. 4 is polar with partial charge in the two iodine atoms (−0.19 in one I atom and +0.12 in the other I atom). Such a change in the charge distribution stems from the complex interplay of molecular structure and solute–solvent interaction. As a result, the polarized I_2 molecule interacts more strongly with the surrounding polar solvent molecules than a neutral one. In terms of the electronic configuration in the molecular orbitals of I_2, this additional charge partially occupies an antibonding σ* orbital and leads to the weakening of the chemical bonding in I_2. In addition, the extra charge filled in the σ* orbital will affect the lowest (bright) electronic excited state, which gives rise to the absorption peak shown in Fig. S1 (ESI†), of I_2 to a larger extent than the ground state because that excited state is reached by the excitation of an electron into the σ* orbital. As a result, the potential energy curve of the lowest (bright) excited state will shift (towards longer I–I bond lengths) by a larger amount than that of the ground state, leading to the increase of the energy difference between the ground state and the Franck–Condon region of the excited state reached by the vertical transition. Therefore, for I_2 in methanol, the optical excitation from the ground state to the lowest (bright) excited state will require photons of larger energies than for I_2 in nonpolar solvents, thus accounting for the solvatochromic blue shift of the absorption spectrum of I_2 in methanol shown in Fig. S1 (ESI†). Here we note recent studies showing that an I_3^- ion adopts an asymmetric structure in protic solvents due to strong solute–solvent interaction and intramolecular charge localization.[33,39,40] The result of the present work indicates that the structure of a neutral I_2 molecule is also affected by the solute–solvent interaction *via* a similar mechanism involving charge localization.

Although we predicted the longer I–I bond in methanol by the quantum chemical calculation, the calculated I–I bond length deviates from the experimental value obtained by the TRXL measurement. In this regard, we note that the configuration of the solute and solvent molecules in Fig. 4 is not the only available solution but rather a snapshot of molecules that fluctuate continuously. In order to examine whether we can predict an I–I bond length value closer to the experimental value, *ab initio* molecular dynamics (AIMD) simulation[39,40] might be needed.

Conclusions

In this work, we investigated the ground-state structure of the I_2 molecule in methanol and cyclohexane solutions using TRXL. By analyzing the TRXL data for I_2 in two different solvents, we elucidated the subtle change in the molecular structure of I_2 induced by the change in solute–solvent interaction. In particular, we found that the I–I bond is longer in methanol than in nonpolar solvents. The longer I–I bond length in methanol is well reproduced by DFT with 22 methanol molecules considered explicitly. Based on the quantum calculations, we propose the molecular origin of the longer I–I bond in methanol, that is, the partial charge developed in an antibonding σ* orbital of I_2 makes the I–I bond weaker and longer. The present results clearly visualize the subtle effect of solute–solvent interaction on the molecular structure.

Acknowledgements

We thank Prof. Shin-ichi Adachi, Prof. Shunsuke Nozawa, and Dr. Tokushi Sato at KEK for helpful discussions. This work was supported by IBS-R004-G2, by the EU grants FAMTO (HPRICT-1999-50004) and FLASH (FP6-503641), as well as by Basic Science Research Program through the National Research Foundation of Korea (NRF) funded by the Ministry of Science, ICT & Future Planning (NRF-2014R1A1A1002511).

Notes and references

1 D. E. Moilanen, D. Wong, D. E. Rosenfeld, E. E. Fenn and M. D. Fayer, *Proc. Natl. Acad. Sci. U. S. A.*, 2009, **106**, 375–380.
2 I. A. Heisler and S. R. Meech, *Science*, 2010, **327**, 857–860.
3 D. Laage, G. Stirnemann, F. Sterpone, R. Rey and J. T. Hynes, *Annu. Rev. Phys. Chem.*, 2011, **62**, 395–416.
4 M. Banno, K. Ohta, S. Yamaguchi, S. Hirai and K. Tominaga, *Acc. Chem. Res.*, 2009, **42**, 1259–1269.
5 D. Roy, S. L. Liu, B. L. Woods, A. R. Siler, J. T. Fourkas, J. D. Weeks and R. A. Walker, *J. Phys. Chem. C*, 2013, **117**, 27052–27061.
6 J. A. Kloepfer, V. H. Vilchiz, V. A. Lenchenkov and S. E. Bradforth, *Chem. Phys. Lett.*, 1998, **298**, 120–128.
7 E. Beckmann, *Z. Phys. Chem.*, 1890, **5**, 76.
8 R. C. Barreto, K. Coutinho, H. C. Georg and S. Canuto, *Phys. Chem. Chem. Phys.*, 2009, **11**, 1388–1396.
9 A. Marini, A. Munoz-Losa, A. Biancardi and B. Mennucci, *J. Phys. Chem. B*, 2010, **114**, 17128–17135.
10 R. S. Mulliken, *J. Am. Chem. Soc.*, 1952, **74**, 811–824.
11 H. Rosen, Y. R. Shen and F. Stenman, *Mol. Phys.*, 1971, **22**, 33–47.

12 J. Yarwood and B. Catlow, *J. Chem. Soc., Faraday Trans. 2*, 1987, **83**, 1801–1814.
13 Y. Danten, B. Guillot and Y. Guissani, *J. Chem. Phys.*, 1992, **96**, 3782–3794.
14 Y. Danten, B. Guillot and Y. Guissani, *J. Chem. Phys.*, 1992, **96**, 3795–3810.
15 U. Buontempo, A. DiCicco, A. Filipponi, M. Nardone and P. Postorino, *J. Chem. Phys.*, 1997, **107**, 5720–5726.
16 W. Kiefer and H. J. Bernstein, *J. Raman Spectrosc.*, 1973, **1**, 417–431.
17 C. Bressler, C. Milne, V. T. Pham, A. ElNahhas, R. M. van der Veen, W. Gawelda, S. Johnson, P. Beaud, D. Grolimund, M. Kaiser, C. N. Borca, G. Ingold, R. Abela and M. Chergui, *Science*, 2009, **323**, 489–492.
18 N. Huse, H. Cho, K. Hong, L. Jamula, F. M. F. de Groot, T. K. Kim, J. K. McCusker and R. W. Schoenlein, *J. Phys. Chem. Lett.*, 2011, **2**, 880–884.
19 S. Nozawa, T. Sato, M. Chollet, K. Ichiyanagi, A. Tomita, H. Fujii, S. Adachi and S. Koshihara, *J. Am. Chem. Soc.*, 2010, **132**, 61–63.
20 S. H. Nie, X. Wang, H. Park, R. Clinite and J. M. Cao, *Phys. Rev. Lett.*, 2006, **96**, 025901.
21 Z. S. Tao, T. R. T. Han, S. D. Mahanti, P. M. Duxbury, F. Yuan, C. Y. Ruan, K. Wang and J. Q. Wu, *Phys. Rev. Lett.*, 2012, **109**, 166406.
22 K. Takemura, S. Minomura, O. Shimomura, Y. Fujii and J. D. Axe, *Phys. Rev. B: Condens. Matter Mater. Phys.*, 1982, **26**, 998–1004.
23 J. Davidsson, J. Poulsen, M. Cammarata, P. Georgiou, R. Wouts, G. Katona, F. Jacobson, A. Plech, M. Wulff, G. Nyman and R. Neutze, *Phys. Rev. Lett.*, 2005, **94**, 245503.
24 H. Ihee, M. Lorenc, T. K. Kim, Q. Y. Kong, M. Cammarata, J. H. Lee, S. Bratos and M. Wulff, *Science*, 2005, **309**, 1223–1227.
25 M. Christensen, K. Haldrup, K. Bechgaard, R. Feidenhans'l, Q. Y. Kong, M. Cammarata, M. Lo Russo, M. Wulff, N. Harrit and M. M. Nielsen, *J. Am. Chem. Soc.*, 2009, **131**, 502–508.
26 H. Ihee, *Acc. Chem. Res.*, 2009, **42**, 356–366.
27 K. H. Kim, J. Kim, J. H. Lee and H. Ihee, *Struct. Dyn.*, 2014, **1**, 011301.
28 K. H. Kim, J. G. Kim, S. Nozawa, T. Sato, K. Y. Oang, T. Kim, H. Ki, J. Jo, S. Park, C. Song, T. Sato, K. Ogawa, T. Togashi, K. Tono, M. Yabashi, T. Ishikawa, J. Kim, R. Ryoo, J. Kim, H. Ihee and S.-i. Adachi, *Nature*, 2015, **518**, 385–389.
29 A. Plech, K. V. M. Lorenc and J. Boneberg, *Nat. Phys.*, 2006, **2**, 44–47.
30 H. S. Cho, N. Dashdorj, F. Schotte, T. Graber, R. Henning and P. Anfinrud, *Proc. Natl. Acad. Sci. U. S. A.*, 2010, **107**, 7281–7286.
31 S. Westenhoff, E. Malmerberg, D. Arnlund, L. Johansson, E. Nazarenko, M. Cammarata, J. Davidsson, V. Chaptal, J. Abramson, G. Katona, A. Menzel and R. Neutze, *Nat. Methods*, 2010, **7**, 775–776.
32 K. H. Kim, S. Muniyappan, K. Y. Oang, J. G. Kim, S. Nozawa, T. Sato, S. Y. Koshihara, R. Henning, I. Kosheleva, H. Ki, Y. Kim, T. W. Kim, J. Kim, S. Adachi and H. Ihee, *J. Am. Chem. Soc.*, 2012, **134**, 7001–7008.
33 K. H. Kim, J. H. Lee, J. Kim, S. Nozawa, T. Sato, A. Tomita, K. Ichiyanagi, H. Ki, J. Kim, S. Adachi and H. Ihee, *Phys. Rev. Lett.*, 2013, **110**, 165505.
34 S. Jun, J. H. Lee, J. Kim, J. Kim, K. H. Kim, Q. Y. Kong, T. K. Kim, M. Lo Russo, M. Wulff and H. Ihee, *Phys. Chem. Chem. Phys.*, 2010, **12**, 11536–11547.
35 A. L. Harris, J. K. Brown and C. B. Harris, *Annu. Rev. Phys. Chem.*, 1988, **39**, 341–366.
36 N. F. Scherer, D. M. Jonas and G. R. Fleming, *J. Chem. Phys.*, 1993, **99**, 153–168.
37 J. H. Lee, M. Wulff, S. Bratos, J. Petersen, L. Guerin, J. C. Leicknam, M. Carnmarata, Q. Kong, J. Kim, K. B. Moller and H. Ihee, *J. Am. Chem. Soc.*, 2013, **135**, 3255–3261.
38 M. Wulff, S. Bratos, A. Plech, R. Vuilleumier, F. Mirloup, M. Lorenc, Q. Kong and H. Ihee, *J. Chem. Phys.*, 2006, **124**, 034501.
39 I. Josefsson, S. K. Eriksson, N. Ottosson, G. Ohrwall, H. Siegbahn, A. Hagfeldt, H. Rensmo, O. Bjorneholm and M. Odelius, *Phys. Chem. Chem. Phys.*, 2013, **15**, 20189–20196.
40 N. K. Jena, I. Josefsson, S. K. Eriksson, A. Hagfeldt, H. Siegbahn, O. Björneholm, H. Rensmo and M. Odelius, *Chem. – Eur. J.*, 2015, **21**, 4049–4055.